Macromolecules

Volume 30, Number 21 October 20, 1997

© Copyright 1997 by the American Chemical Society

Molecular Weight Effects on Polystyrene Fingerprint Time-of-Flight Secondary Ion Mass Spectrometry (ToF-SIMS) Spectra

X. Vanden Eynde* and P. Bertrand

Unité de Physico-Chimie et de Physique des Matériaux (PCPM), Université Catholique de Louvain, Place Croix du Sud 1, 1348 Louvain-la-Neuve, Belgium

R. Jérôme

Center for Education and Research on Macromolecules (CERM), University of Liège, Bat. B6, Sart-Tilman, B-4000 Liège, Belgium

Received February 14, 1997; Revised Manuscript Received July 7, 1997[⊗]

ABSTRACT: Monodisperse polystyrenes (PS) of different molecular weights (M_n) synthesized by living anionic polymerization with three types of butyllithium initiator (linear, *n*; secondary, *sec*; and tertiary, *tert*) were analyzed by ToF-SIMS (time-of-flight secondary ion mass spectrometry). The influence of the molecular weight on the secondary ion intensities was studied in detail for the fingerprint part of the mass spectra (with $m/z < 200$). A drastic effect was observed for M_n values below 10^4, related to the presence of the saturated butyl end group. An extra hydrogen transfer originating from this end group during the secondary ion formation must be invoked to explain the data. Only the first neighbor monomer repeat units seem to be affected. This H exchange increases the intensity of ions containing more hydrogen or needing H transfer for their formation as the tropylium ion ($C_7H_7^+$ at $m/z = 91$). The molecular structure of the butyl end group is found to influence greatly not only the intensity of their parent ion but also the PS characteristic ion intensities. Indeed, the *tert*-butyl end group is seen unable to produce the H transfer observed for the *n*- and *sec*-butyl ones. A model is proposed to take the influence of the end group on the PS SIMS fragmentation pattern into account. The parameters of this model allow the quantification of the end group interaction.

Introduction

Secondary ion mass spectrometry in the static mode (SSIMS) is becoming an important technique to characterize polymer surfaces.[1] This is due to the very specific chemical information obtained from the detection of characteristic patterns of secondary molecular ions resulting from the macrochain fragmentations. These patterns exhibit distinct fingerprints for the different polymers[2] and the molecular composition and structure of the ions can be related to the polymer original structure (precursor).[2] This fingerprint nature of the SSIMS spectra allows the technique to be used for the study of the surface of various systems like copolymers, polymer blends, and plasma-deposited polymers, such as the surface modifications caused by plasma treatments, material processing, additives segregation, contamination.... The technique is very sensitive to the topmost surface layers and an information depth lower than 10 Å has been recently determined for molecular ions.[3]

However, the quantitative interpretation of the spectra that is needed for the quantification of the surface composition based on SSIMS analysis is still in its infancy. Recent studies have shown that matrix effects seem to be much less important for polymers analyzed in the static mode than for inorganic material analyzed in the dynamic mode.[4] To progress in this field, it is important to be able to identify the different pathways starting from the precursor macromolecules up to the formation of a specific secondary fragment ion.[5−7]

The aim of this paper is to study the influence of the polymer molecular weight on the secondary ion intensities. Indeed, the contribution of the chain ends is expected to become more and more important when the molecular weight decreases.

* E-mail: vandeneynde@pcpm.ucl.ac.be.

[⊗] Abstract published in *Advance ACS Abstracts,* September 15, 1997.

S0024-9297(97)00204-0 CCC: $14.00 © 1997 American Chemical Society

Polystyrene (PS) has been chosen for this study because, on the one hand, monodisperse material with controlled molecular weight can be synthesized by living anionic polymerization and, on the other hand, its spectrum is well-known. It mainly consists of aromatic ions produced by rearrangements between the main chain and the lateral phenyls. The structures have been determined by isotopic labeling[8,9] and by tandem mass spectrometry.[5]

It is well-known that, for PS, intact oligomer emission can be produced by cationization with a substrate atomic ion if low molecular weight polymer monolayers are deposited onto a metallic surface (silver is the most often used). This allows the direct determination of the molecular weight parameters: molecular weight distribution (MWD); number average (M_n) and weight average (M_w) molecular weight of the macromolecules.[10] Also using this method, the identification and the quantification of end groups can be performed.[11] But for thick films and bulk samples of practical interest that are considered in this work, the entanglement of the polymer chains prevents this direct oligomer emission and only small fragments of the polymer are emitted (fingerprint).[10]

The effects of the molecular weight on the fingerprint spectra have been already studied by several authors.[12−16] It was found that, for polystyrene, an effect is detected only for $M_n < 50000$. Below this limit and depending on the considered fragment ion, either a decrease or an increase or no change of the relative ion intensity was found with the decrease of M_n.[12] The dependence of the normalized intensities was shown to be related to the hydrogen content of the ion. It decreases with M_n for the hydrogenated ions and it increases for the more dehydrogenated ones. A similar M_n limit, ranging between 50 000 and 94 000 was reported for poly(lactic acid) surfaces by Shard et al.[13] They observed, for H-terminated polymers, an increase of the (M + H)/(M − H) intensity ratio when M_n decreases below the limiting value, M being the lactic acid (LA) repeat unit. Moreover, the M_n limit can be shifted by surface segregation of specific end group functionality. Similar molecular weight effects were recently shown for poly(methyl methacrylate) (PMMA) by Leeson et al.[16]

In this work, only butyl end groups with different types of branching are considered. It is worthwhile to recall that end groups play an important role in polymer properties such as reactivity for copolymerization, graft polymerization, polymer miscibility, and compatibility with external compounds (biocompatibility, adhesion) and also in processing capabilities. PS end groups containing heteroatoms have already been studied elsewhere.[17]

Experimental Section

Materials. Monodisperse polystyrenes with different molecular weights were synthesized by living anionic polymerization at the Center for Education and Research on Macromolecules, Liège University.[18] Three types of butyl initiator were used: linear (*n*), secondary (*sec*), and tertiary (*tert*) butyllithium (see Chart 1). The number (M_n) and weight (M_w) average molecular weights and the polydispersity ratio ($H = M_w/M_n$) were measured by GPC for the different samples, and the values are listed in Table 1. Owing to the almost monodispersity of the samples, only the number average molecular weights M_n are considered below.

Methods. Sample Preparations. All thin film samples were prepared by spin coating (5000 rpm spinning) a drop of solution (30 mg/mL in toluene, HPLC grade solvent from Union Chimique Belge) onto a silicon wafer. No further

Chart 1. PS Chemical Structures: *sec*-Butyl (a), *n*-Butyl (b), and *tert*-Butyl (c) End Groups

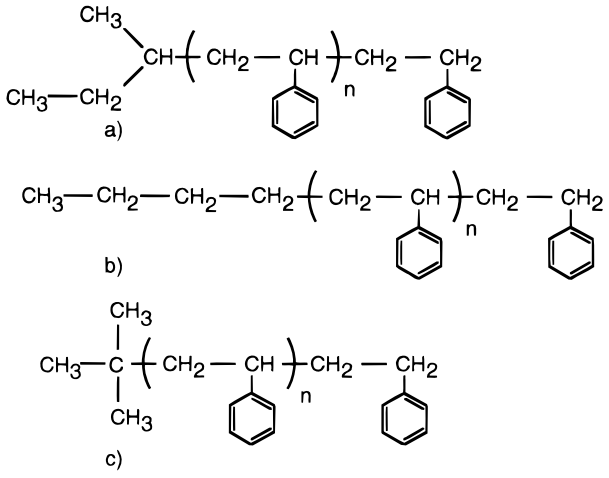

Table 1. M_n, M_w, and H Measured by GPC for Monodisperse Polystyrene

	M_n	*n* (mol)	M_w	H
s-850	850	7	953	1.12
s-3650	3644	34	3829	1.05
s-3750	3756	35	3946	1.05
s-6460	6458	61	6756	1.05
s-8700	8694	83	9078	1.05
s-10200	10181	97	10623	1.04
s-1630[a]	1630	15	1780	1.09
s-2180[a]	2180	20	2306	1.08
s-4760[a]	4760	45	5110	1.07
s-8000[a]	8000	76	8400	1.05
s-12400[a]	12400	118	13200	1.06
s-18100[a]	18100	173	19300	1.07
n-3400	3391		4384	1.29
n-5200	5180		6958	1.34
n-9000	8979		12120	1.35
t-2000	2085		2418	1.16
t-3500	3457		5198	1.23
t-10600	10599		11571	1.09

[a] Results of the first set of measurements.

treatment was applied before analysis. All films were free of cracks and defects and were thick enough (≥∼5 nm) to avoid the silicon signal (Si, 28 *m/z*) in the SSIMS spectra originating from the substrate.[3] All samples were free of additives and small molecular weight compounds and indeed no contribution from them is found in the spectra.

ToF-SIMS. The static SIMS measurements were carried out at UCL, Louvain-la-Neuve, by means of a Charles Evans & Associates TFS-4000 MMI time-of flight spectrometer using a $^{69}Ga^+$ (15 keV) liquid metal ion source.[19] In this system, the secondary ions are accelerated at 3 keV before being 270° deflected by three electrostatic hemispherical analyzers (TRIFT).[19] A 530 pA dc primary ion beam is pulsed at a 5 kHz frequency with a pulse width of 4 ns and is rastered over a 100 × 100 μm^2 surface area. All spectra were acquired during 10 min with a fluence $<10^{12}$ ions/cm^2, ensuring static conditions. A mass resolution $m/\Delta m$ of ∼3000 measured at 28 *m/z* on a Si wafer was achieved. No charge neutralization was needed.

Data Treatments and Normalization. (I) Normalization of the Spectra. All the spectra treatments were made with the Cadence 1 software from Charles Evans & Associates. For each of the peaks contributing to the spectrum (*b*), the absolute intensity $Y^b_{ABS}(i)$ was measured and a unique ion composition was assigned (*i*). In order to get rid of the fluctuations of the absolute intensities when comparing spectra recorded at different periods of time, all intensities were normalized ($Y^b_{NORM}(i)$) with respect to the total intensity (I^b_{Total}) in the spectrum (*b*) from which were substracted the hydrogen intensity ($Y^b_{ABS}(H)$) and the sum of all contaminant

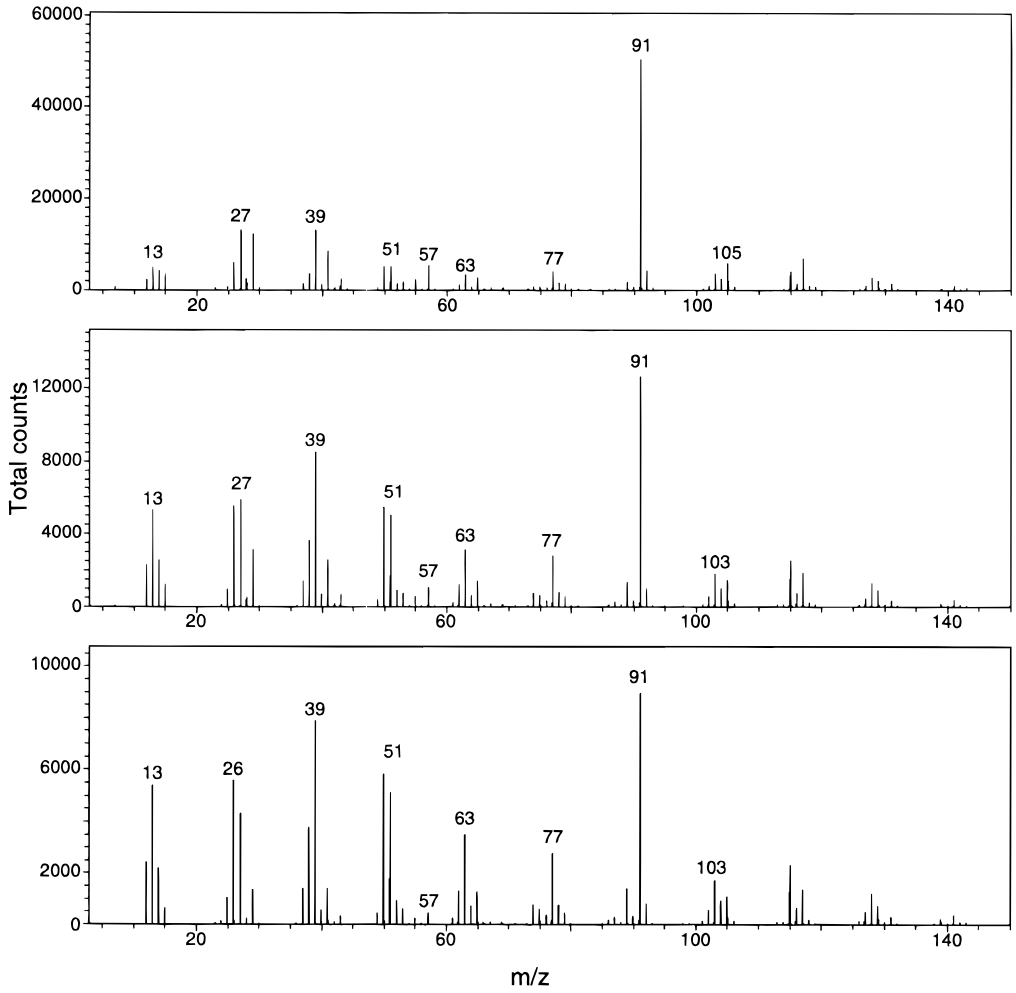

Figure 1. ToF-SIMS spectra (*m*/*z* from 5 to 150) of monodisperse polystyrenes with M_n = 850 (top), 3750 (middle), 10 200 (bottom).

intensities ($\sum Y^b_{ABS}$(Cont)) (see eq 1). Indeed, the spectra of two series of samples of the *sec*-butyl PS were recorded at two different periods of time. The first set of samples was the series "s*" in Table 1 and the second set was the series "s".

$$Y^b_{NORM}(i) = \frac{Y^b_{ABS}(i)}{I^b_{Total} - \sum Y^b_{ABS}(\text{Cont}) - Y^b_{ABS}(\text{H})} \quad (1)$$

The reproducibility of the normalized intensity was tested by measuring the standard deviation for each variable (ion *i*) by means of at least four independent measurements (spectrum *b*). A standard deviation of ~5% of mean normalized intensity was found.

For the contaminants, only low intensities were measured, which were mainly poly(dimethylsiloxane) (PDMS) with contributions at *m*/*z* = 28 (Si^+), 43 ($SiCH_3^+$), 73 ($[Si(CH_3)_3]^+$), and 147 ($[(CH_3)_3SiOSi(CH_3)_2]^+$) and alkali cations such as lithium (Li^+ at 6 and 7 *m*/*z*), sodium (Na^+ at *m*/*z* = 23), potassium (K^+ at *m*/*z* = 39), and chlorine (Cl^- at *m*/*z* = 35 and 37). The Li peaks originated from the polymerization initiator.

(II) Absolute Intensity Consideration. In order to examine the variations of absolute intensity $Y^b_{ABS}(i)$ relative to one ion (*i*), its deviation ($Y^{b\prime}_{ABS}(i)$) with respect to its mean value averaged over *t* spectra $[(1/t)\sum_{b=1}^{t} Y^b_{ABS}(i)]$ was evaluated (see eq 2).

$$Y^{b\prime}_{ABS}(i) = \frac{Y^b_{ABS}(i) - \frac{1}{t}\sum_{b=1}^{t} Y^b_{ABS}(i)}{\frac{1}{t}\sum_{b=1}^{t} Y^b_{ABS}(i)} \quad (2)$$

This data transformation avoids considering the absolute intensity differences between ions but it allows the comparison of the intensity variations according to one parameter, molecular weight in our case. Equation 2 can be used if for each molecular weight (or sample), the same number of spectra is involved in the calculation. Otherwise, every spectrum has to be weighted by the number of spectra measured for each particular molecular weight. Nevertheless, this requires a reproducibility of the total intensity (I_{Total}) when the same sample is measured many times. This can be more easily realized with the spin-coated thin films.

Results

The results are presented in two parts. First, *sec*-butyl PS spectra are considered. The influence of the molecular weight on the normalized and absolute intensities is presented and discussed in parts Ia and Ib, respectively. Then, in part II, the influence of the butyl initiator isomer type (n, s, t) is investigated.

Part I. Molecular Weight Effects for *sec*-Butyl PS. (a) Normalized Intensities. Since most of the information on the PS surfaces is contained in the positive spectrum, the presentation is restricted to these data.

The PS ToF-SIMS spectra (Figure 1) are similar to those previously published[2] except for the peak intensity ratios that will be discussed in detail below. No traces of oxidation or additives were detected in the spectra.

The influence of the molecular weight on the total intensity of the spectrum is presented in Figure 2 for the two sets of samples. An important increase of I_{Total} is observed for M_n < 10 000. This increase influenced

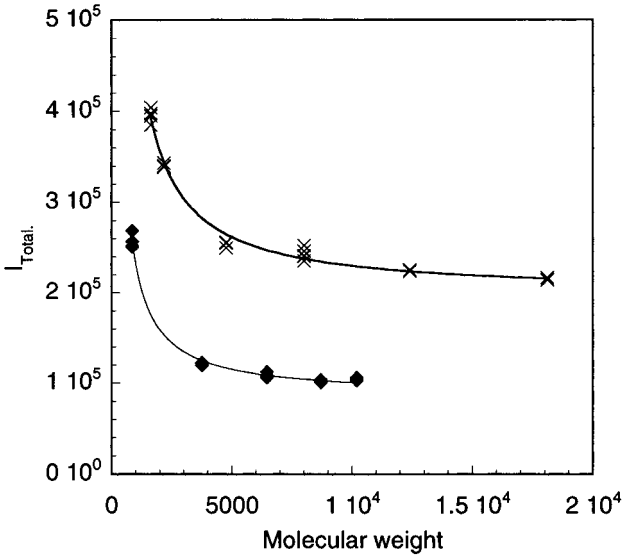

Figure 2. Total intensity (I^b_{Total}) versus number average molecular weight (M_n). The two runs of data are represented (s and s* data set are labeled with black boxes and crosses, respectively).

all the normalized intensity values calculated by eq 1. This is discussed in part Ib.

All the peak intensities were found to remain constant when the molecular weight was increased above the limit of 10 000. This limit was somewhat lower than the one determined in our previous work (50 000).[12] This was made possible since the samples investigated here had lower molecular weights, falling within narrower limits than those previously studied.

A careful treatment of the normalized spectra led to three different characteristic behaviors for the ion intensity versus M_n. When the molecular weight increases, the normalized intensity of an ion either increases (type I, see Figure 3a for $C_2H_2^+$) or is almost constant (type II, see Figure 3b for $C_8H_7^+$) or decreases (type III, see Figure 3c for $C_7H_7^+$), confirming the results presented in ref 12.

All the ions in the spectra can be classified along these three types of dependence vs M_n, as shown in Table 2. The three types of ions are observed in every carbon cluster C_x (group of ions containing an identical number (x) of carbon atoms in their molecular structures), and they depend within one cluster on the number (y) of H atoms. As may be seen from Table 2, within each cluster, type I is observed for ions with lower H content y (the more unsaturated ions); type III, for ions with the higher H contents (more hydrogenated), and type II for ions with medium number of H.

The normalized intensity of ion $C_4H_9^+$ ($m/z = 57$) is shown in Figure 4. This saturated ion is not characteristic of the PS molecular structure, but it is the parent ion of the *sec*-butyl initiator end group.[12,20] Its intensity increases with the molecular weight decrease (type III). The supplementary intensity for low molecular weight cannot be due to initiator residues from the anionic polymerization process. Indeed, any remaining butyl reacts with protons during the termination step forming butane. The fragmentation of this end group produces saturated daughter ions such as CH_3^+ ($m/z = 15$) and $C_2H_5^+$ ($m/z = 29$) (see Chart 2), and rearrangement and/or further fragmentation reactions can lead to other highly hydrogenated ions like $C_3H_5^+$ ($m/z = 41$) and $C_3H_7^+$ ($m/z = 43$), which are all of type III. The behavior of the butyl ion can be explained by invoking

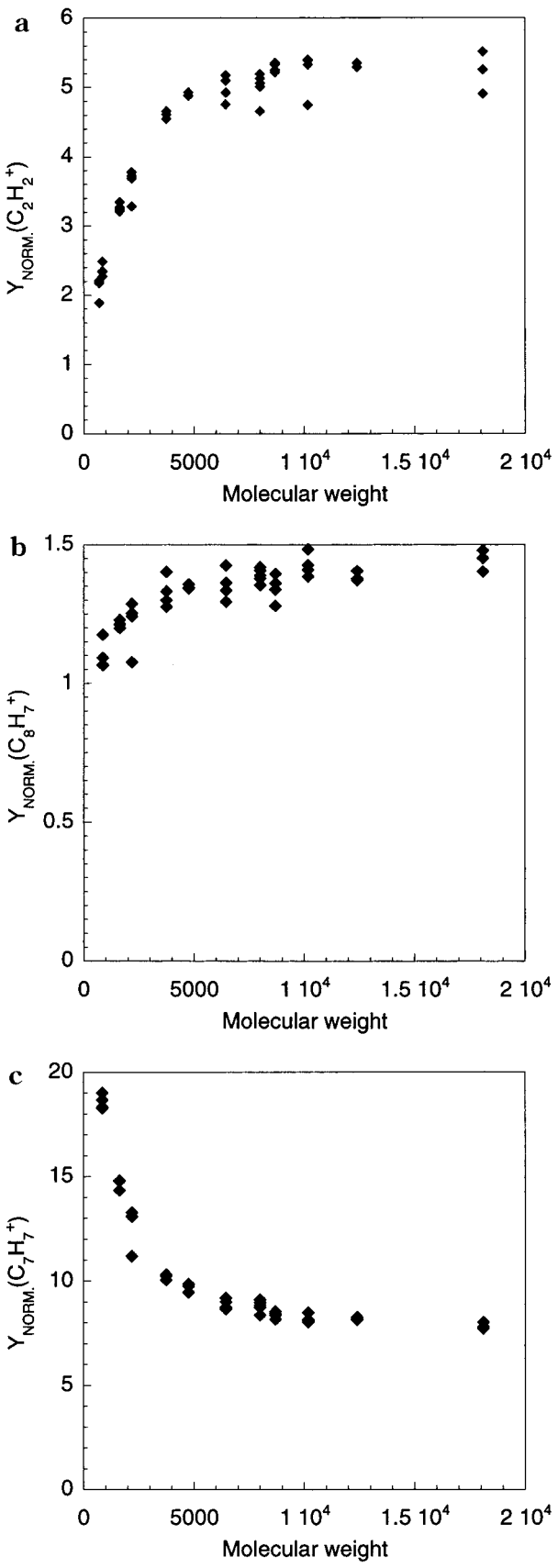

Figure 3. Typical behaviors $Y^b_{\text{NORM}}(X)$ vs molecular weight: (a) type I ion, $C_2H_2^+$ (26 m/z); (b) type II ion, $C_8H_7^+$ (103 m/z); (c) type III ion, $C_7H_7^+$ (91 m/z).

an increasing surface concentration of end groups when the molecular weight is lowered. A preferential surface segregation of the end group could also contribute to

Table 2. Different Dependence Types of the C_xH_y Ion Intensities on the Molecular Weight

x	type I	*y*	type II	*y*	type III	*y*
1	13	1			15	3
2	26	2			27, 29	3, 5
3	39	3	40	4	41, 43	5, 7
4	51	3	53	5	57	9
5	63	3	65	5		
6	77	5	78	6		
7	89	5	90	6	91	7
8			103	7	105	9
9	115	7	116	8	117	9
10	127	7	128	8	131	11

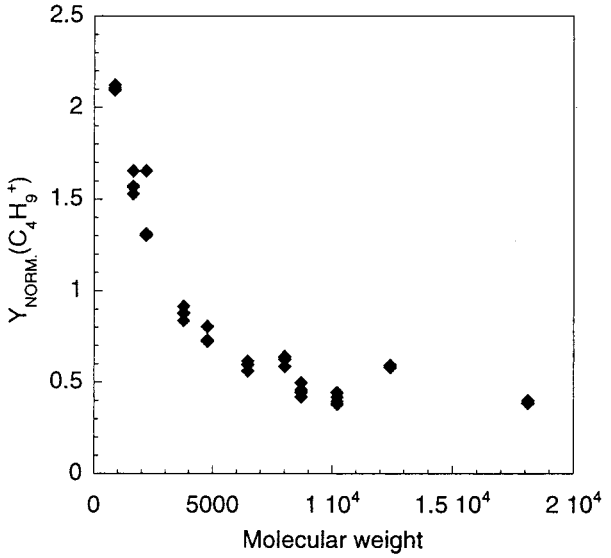

Figure 4. Normalized intensity of $C_4H_9^+$ (57*m*/*z*) ($Y^b_{NORM}(C_4H_9^+)$) vs molecular weight.

Chart 2. Fragmentation of the *sec*-Butyl End Group

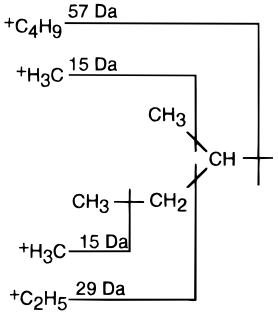

enhance this effect. Indeed, an end group surface segregation could be driven by the higher entropy of the butyl as compared to the chain or to the styrene end group.

The direct emission and the fragmentation of the saturated end group cannot account for the type III ions heavier than $m/z = 57$. However, the three types of behaviors are still observed within the clusters higher than C_4. For the low molecular weight PS, the *sec*-butyl presence is then believed to be the source of hydrogen (or proton) transfer that favors the formation of additional hydrogenated ions of type III.

The most characteristic ions of polystyrene ($m/z = 77$, 103, 105, 115, 141, 165, ...) are seen to be of type I or II except for the tropylium ion ($C_7H_7^+$, $m/z = 91$), which is type III, as shown in Figure 3c. The formation of this ion requires a rearrangement reaction between the phenyl pendant ring and the α C atom of the backbone accompanied by the addition of an H coming from the β carbon.[8] The increase of the tropylium normalized intensity with decreasing M_n shows that this H transfer is favored by the presence of the saturated butyl end group.

Scheme 1. H Exchange for $C_7H_7^+$ Formation: From the Main Chain (Dashed Lines)[9] (a and b) or with the Butyl End Group Interaction (a) (Solid Lines)

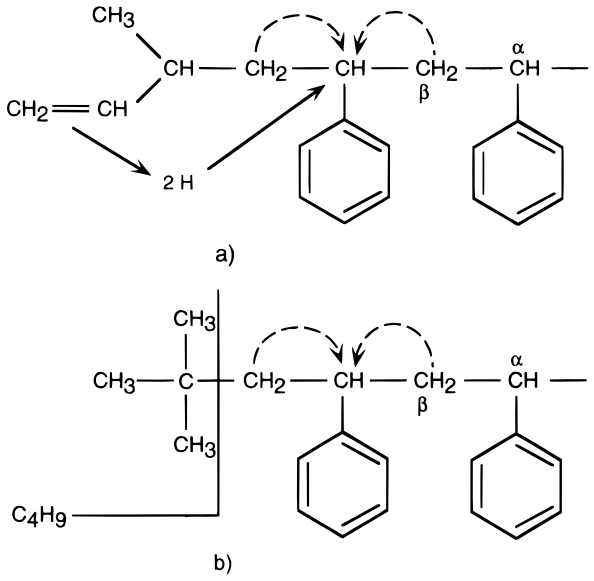

The origin of the increase of the tropylium intensity is due to a specific interaction between the initiator end group and phenyl of the adjacent monomer unit. Indeed, the H atoms of the alkyl end group could be the source of the H transfer required for the formation of the tropylium ion and other less unsaturated species (Scheme 1). Hittle et al. have shown[14] that this H (or D for deuterated PS) exchange is possible with an intramolecular process and that no intermolecular exchange is observed. Moreover, a comparison between results from random[9] and block[21] copolymers of hydrogenated and deuterated PS have shown that H/D exchange during the secondary ion formation occurs only significantly for random copolymers. This suggests that only the adjacent monomer units are involved in the H exchange. It is worth noting that hydrocarbon contamination cannot be excluded as a possible source for H exchange, but this effect would be negligibly small.

As the size of the PS fragments increases, the effect of molecular weight decreases and type II ions become more and more unsaturated. Then the hydrogen exchange mechanism can be extended to all low-weight fragments of polystyrene. Some originally unsaturated fragments can catch an H atom (or proton) and become more saturated. This possibility is examined in the model proposed in the discussion part.

Leggett et al. proposed a model for the formation of the PS fragments based on tandem mass spectrometry results.[5] In this model, the $m/z = 77$ ($C_6H_5^+$) ion generates, after gas phase collisions, daughter ions at $m/z = 76$ ($C_7H_6^+$), 51 ($C_4H_3^+$), and 39 ($C_3H_3^+$). The tropylium $m/z = 91$ ion breaks into $m/z = 65$ ($C_5H_5^+$), 63 ($C_5H_3^+$), 51, and 39 daughter ions but cannot be generated by any other fragment of the PS in the MS−MS experiments. The $m/z = 103$ ($C_8H_7^+$) ion has daughter ions at $m/z = 77$, 51, and 39.

According to our classification, the $m/z = 77$ ion and all its daughter ions belong to the same type I, whereas the $m/z = 91$ ion is of type III while all its daughter ions are of other types. The $m/z = 103$ ion is of type II

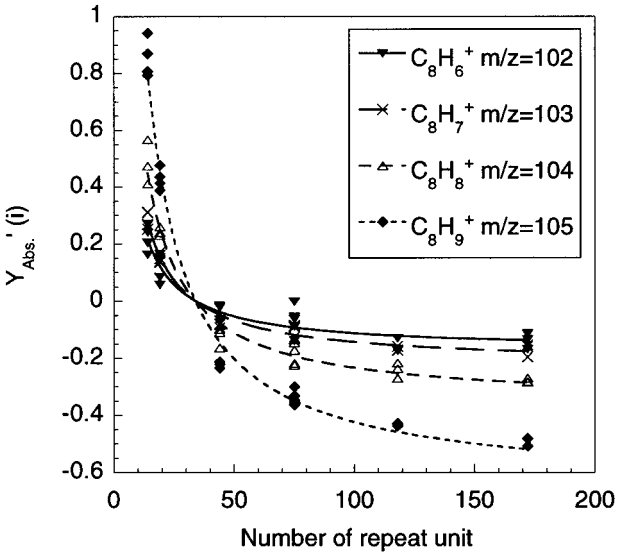

Figure 5. Absolute intensities of C_8 cluster ($Y^{b\prime}_{ABS}(i)$) vs molecular weight.

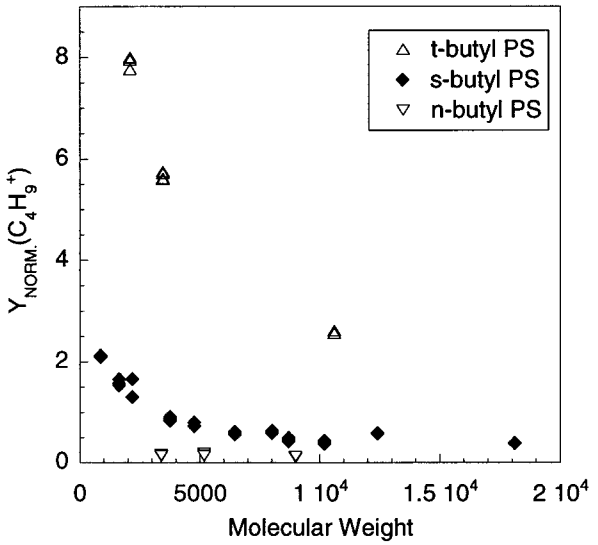

Figure 6. Normalized intensities of $C_4H_9^+$ ions (57 *m*/*z*) ($Y^{b}_{NORM}(C_4H_9^+)$) vs molecular weight with the different initiators.

or slightly decreasing with increasing M_n, but its daughter ions are of type I (see Table 2). Since some parent ion behaviors do not show any influence on their daughter ions, we can assume that there exist additional pathways for the fragmentation of PS when M_n is small. These pathways are related to the presence of the end groups at the surface. Moreover, this could also explain the different behaviors observed for the parent and daughter ions of Leggett's scheme.[5]

(b) Absolute Intensities. When the normalized intensity obtained by eq 1 is considered, three types of ion behaviors have been observed. Considering, now, the absolute intensities, only the results obtained during the same run relative to the first set of samples (Table 1, series "s*") are presented and discussed. Figure 5 shows $Y^{b\prime}_{ABS}(i)$ (eq 2) vs M_n for ions in the C_8 cluster. Only two types of M_n dependencies are observed for the intensity: either there is no variation as for the $C_8H_6^+$ ion (eq 2) with its corrected absolute intensity values close to zero, A type, or it increases at low M_n as for the $C_8H_7^+$ ion, B type. In the latter case, the increase for the C_8 follows the sequence $C_8H_6^+ < C_8H_7^+ < C_8H_8^+ < C_8H_9^+$. In all the other clusters of the PS spectra (from C_1 to C_{11}), similar behaviors are observed. Type A is observed for the most dehydrogenated ions, indicating that there is no effect of M_n on their intensity. The more H atoms are contained in the ion structure, the more important is the increase of $Y^{b\prime}_{ABS}(i)$ for low molecular weight samples, as shown in Figure 5.

It is evident that the three types of behavior observed for the normalized intensities come from the normalization procedure itself. A decrease of $Y^{b}_{NORM}(i)$ is indeed produced if the absolute intensity $Y^{b}_{ABS}(i)$ is constant or grows slower than I^{b}_{Total} when M_n decreases. Thanks to the good reproducibility obtained during each run of measurements, it is possible to model directly the absolute intensity variations (see the Discussion). The interpretation on the fragmentation pathways in SIMS should be based on absolute intensity values.

Part II. Influence of the End Group Isomeric Structure. The influence of the end group isomeric structure is investigated by comparing the results obtained for *n*-butyl, *sec*-butyl, and *tert*-butyl. Since the absolute intensities are not directly comparable because these samples were analyzed during different runs, only the normalized intensities are compared. Figure 6 presents the butyl ($C_4H_9^+$, 57 *m*/*z*) normalized intensity variation vs M_n. It may be seen that, for the same M_n, Y_{NORM} increases following the sequence *n*-butyl < *sec*-butyl < *tert*-butyl. This sequence is the same as for the heat of formation and for the ionization potential (see Table 3). For ions with a molecular structure similar to that of the end group, the SSIMS intensity is expected to be higher for branched ions since they are more stable due to the inductive effect of alkyl groups stabilizing the carbonium ion. In mass spectrometry, a compound with a higher ionization energy gives more neutral species (case of *n*-butyl) than those with lower ionization energy (case of *tert*-butyl).[22] A similar effect of the butyl isomers was observed for poly(butylmethacrylate).[23] However, a primary carbonium ion could rearrange to stabilize its structure and give a secondary carbonium ion, but this is not likely to occur in the case of butyl ions. The inductive effect is larger for *tert*- and *sec*-butyl than for *n*-butyl, which contributes to produce a more stable secondary ion. For *n*-butyl, the normalized intensity is seen to be very low and nearly constant. This shows that most of the intensity of the 57 *m*/*z* peak should unambiguously be ascribed to the presence of the initiator end group. Another explanation could be the competition between the H transfer and the secondary emission of a butyl fragment. Indeed, if the butyl end group interacts with the first monomer unit to emit a PS fragment, its emission is no longer possible.

Table 3. Properties of the C_4H_9 Ions[27]

	ionization potential (eV)	heat of formation ΔH_f (kJ/mol)
n-C_4H_9	8.02	849
s-C_4H_9	7.25	766
t-C_4H_9	6.7	694

For high molecular weight samples, the normalized intensities converge all toward the same value, independently of the isomer structure. This means that the contribution of *n*-butyl end groups to the 57 *m*/*z* intensity is negligible and most of it is due to the main chain. A contribution due to the contamination should be excluded, since it is unlikely that it would have a similar effect for the three series of samples.

Concerning the influence of the end group isomericity on the other ions of the PS spectra, the M_n dependencies

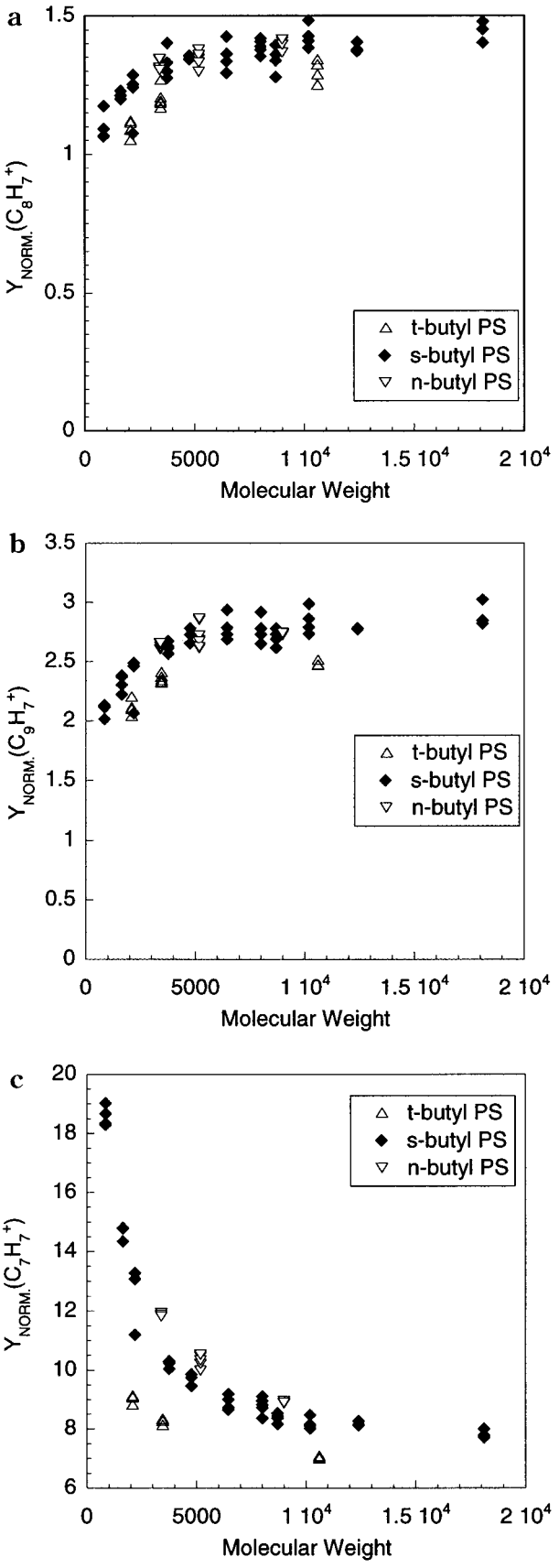

Figure 7. Normalized intensities with the different initiators, $Y^{b}_{NORM}(X)$ vs molecular weight: (a) $C_8H_7^+$ at $m/z = 103$; (b) $C_9H_7^+$ ions at $m/z = 115$; (c) $C_7H_7^+$ ions at $m/z = 91$.

were found to be similar, independently of the end group. For PS characteristic ions ($m/z = 26$, 39, 51, 77, 103, 105, 115) (see Figure 7), *n*-butyl and *sec*-butyl end groups give similar values. For the *tert*-butyl end group, all the normalized intensities (except for 39 m/z) are lower than for the *n*- and *sec*-butyl PS. These low normalized intensities for the aromatics and unsaturated peaks are compensated for by the increase of saturated ions ($m/z = 15$, 29, 41, 57) originating from the *tert*-butyl fragmentation.

Scheme 2. Macromolecule Model

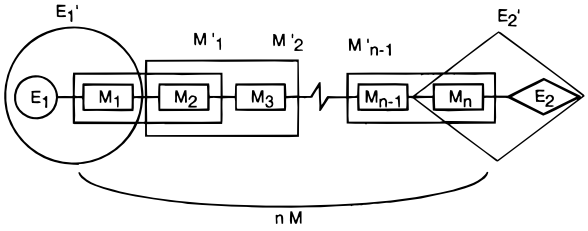

The tropylium $C_7H_7^+$ normalized intensities of *n*- and *sec*-butyl (Figure 7c) are very similar. For *tert*-butyl, the increase at low M_n is much weaker. It appears that the *tert*-butyl end group has a lower influence on the promotion of the tropylium formation than the *n*- and *sec*-butyl. This can be attributed to a most favorable path for the formation of the $C_4H_9^+$ that avoids the rearrangement of the end group leading to the fragment $C_7H_7^+$ at 91 m/z. Indeed, the H transfer from the butyl group to the next PS repeat unit can be hindered in the case of the *tert*-butyl because, with its double branching, it has no first neighboring H to be transfered, as is the case for *n*- and *sec*-butyl (Scheme 1). In mass spectrometry, this mechanism is called a 1,2 hydrogen shift. Another explanation could be the McLafferty rearrangement[22] taking place with a *sec*-butyl end group but not with the *tert*-butyl. Indeed, the H transfer through the six-membered ring transition state involving the end group and the first monomer unit is favored for the less branched butyl end group.

Discussion

In order to account for the observed intensity dependencies with M_n, a simple model is proposed. The structure of linear polymer macrochains is modeled as an ensemble of ($n + 2$) linked "molecules" (see Scheme 2). The first and last ones contain the end groups (E_1 and E_2) and the n others, the monomer repeat unit (M_i with $i = 1$ to n). Although in our *sec*-butyl PS, only one end group is different than the styrene unit, the other being of the same type as the monomer repeat unit (H ending), it may contribute differently to the spectrum than the other repeat units. Indeed, only one backbone breaking is required to produce fragments from it, and this is expected to yield higher intensities. However, we have shown that the influence of the second end group is negligible in the spectra of *sec*-butyl PS ended with a hydrogenated styrene unit or an alcohol functionality.[12]

The molecular weight for a perfect monodisperse polymer ($H = 1$) is given by

$$M_n = n m_M + m_{E_1} + m_{E_2} \qquad (3)$$

where m_M is the molecular weight of one monomer repeat unit (104 g/mol for PS), m_{E_1} is the molecular weight of the first end group functionality (57 g/mol for *sec*-butyl), m_{E_2} is the molecular weight of the second end group (last repeat unit, M + H in our case), and n is the number of repeat units in the polymer macrochain of molecular weight M_n.

If molar fractions are considered, one obtains for end groups (f_{E_i}, $i = 1$ or 2) and repeat units (f_M), respectively

$$f_{Ei} = \frac{1}{n+2} \tag{4}$$

$$f_M = \frac{n}{n+2} \tag{5}$$

When a surface, considered homogeneous in the analyzed area A, contains only one kind of molecule M with a surface concentration n_M, the basic relationship for the absolute intensity (Y_X) of one specific ion (X) (in number of detected ions in the static SIMS spectrum) is given by[24]

$$Y_X = An_m F\sigma_M P(M\rightarrow X)T \tag{6}$$

where F is the incident ion fluence, $\sigma(M)$ is the sputtering/desorption cross-section for the molecule M, and $P(M\rightarrow X)$ is a transformation ratio, expressing the average number of ions X generated by the disappearance of one molecule M and emitted in the solid angle accepted by the spectrometer. T is an experimental factor taking into account the spectrometer transmission and the detector efficiency.

If the surface contains different types of molecules, M (end groups, monomer repeat units), with molar fractions f_{E_i} and f_M, respectively, and if no matrix effect applies, eq 6 becomes

$$Y_X = f_{E_1} Y_{E_1,X} + f_M Y_{M,X} + f_{E_2} Y_{E_2,X} \tag{7}$$

where $Y_{E_i,X}$ are the intensities of ion X measured on a hypothetical sample containing only E_i molecules, and $Y_{M,X}$ is the intensity for a polymer of infinite molecular weight M_n.

For our modeled polymer, this gives

$$Y_X = \frac{1}{n+2}(Y_{E_1,X} + Y_{E_2,X}) + \frac{n}{n+2} Y_{M,X} \tag{8}$$

This equation applies for all ion intensities in the spectrum on the condition that no formation of the ion, X, requires the disappearance of more than one repeat unit M or $E_i + M$ molecules; otherwise the definition of M and E_i have to be modified accordingly. Of course, terms have to be added in eq 8 with the correct concentration coefficients if contaminants are present. For butyl-ended PS, the first term of eq 8 vanishes for fragments X with $m/z > m/z(E_1) = 57$. If some ions are only specific of the end group, then the last term vanishes. Recent results obtained for deuterated PS have shown that this is indeed the case for the saturated ion $X \equiv E_1$ at $m/z = 57$.[25]

With this formalism, the influence of the molecular weight (n) on the total intensity I_{Total} and hence on the normalization procedure (eq 1) is then obvious:

$$I_{TOTAL} = \sum_i [Y_X] = \sum_i \left[\frac{1}{n+2} Y_{E_1,X} + \frac{n}{n+2} Y_{M,X} + \frac{1}{n+2} Y_{E_2,X}\right] \tag{9}$$

where the summation is made over all ions in the spectrum.

$$I_{TOTAL} = \frac{1}{n+2}[\sum_i Y_{E_1,X} + \sum_i Y_{E_2,X}] + \frac{n}{n+2}\sum_i Y_{M,X}$$

For high molecular weights, we can assume that n is infinity. This gives

$$\lim_{n\to\infty} I_{TOTAL} = \sum_i Y_{M,X} = B$$

Whereas for a hypothetical molecule with no repeat unit but only end groups, n is close to zero:

$$\lim_{n\to 0} I_{TOTAL} = \frac{1}{2}[\sum_i Y_{E_1,X} + \sum_i Y_{E_2,X}] = A$$

Equation 9 may be rewritten in a short form:

$$I_{TOTAL} = \frac{2}{n+2} A + \frac{n}{n+2} B \tag{9b}$$

The term B is strictly related to the main chain ions. By constrast, the term A is related to the influence of the end groups on the ion yield of X species. The fit of I_{TOTAL} by eq 9b is shown in Figure 2 for both data sets. It is observed that the variation is well described by the model whatever the considered data set.

The peak intensity ratio (Y_{X_1}/Y_{X_2}) obtained by eq 8 can be simplified under the following hypotheses: (a) only one end group E_1 contributes to the intensity of X_1, and (b) only the main chain M contributes to the intensity of X_2. Then

$$\frac{Y_{X_1}}{Y_{X_2}} = \frac{1}{n+2}\frac{Y_{E_1,X_1}}{Y_{M,X_2}} \tag{10}$$

This relation has already been proposed by Reihs et al.[14]

In order to model the extra hydrogen exchange due to the interaction of the first repeat unit with the neighboring butyl end group (this can lead to the increase in the intensity of some ions, as seen for the tropylium in the Results), the transformation ratio $P(M\rightarrow X)$ defined in eq 6, has to be modified by a factor α for the ions produced by this first repeat unit. As already discussed, the influence of the end group is assumed to be limited to its first neighboring molecule M. If a H transfer is favored for the formation of the considered ion, then $\alpha > 1$.

The intensity of ion X is then modified as

$$Y_X = \frac{1}{n+2}(Y_{E_1,X} + Y_{E_2,X}) + \frac{n-1+\alpha}{n+2} Y_{M,X} \tag{11}$$

and, as for I_{TOTAL},

$$\lim_{n\to\infty} Y_X = Y_{M,X} = B$$

$$\lim_{n\to 0} Y_X = \frac{1}{2}[Y_{E_1,X} + Y_{E_2,X}] + \frac{\alpha-1}{2} Y_{M,X} = A'$$

or

$$Y_X = \frac{2}{n+2} A' + \frac{n}{n+2} B \tag{12}$$

Whatever the assumptions on the end group interaction, eq 12 will be valid. All end group interaction contributions to one given ion intensity are contained in the terms A' and for the main chain ions in the term

B. The ratio A'/B of both terms is characteristic of the influence of the end group on the absolute intensities of all ions in the spectrum.

$$\frac{A'}{B} = \frac{1}{2}\frac{[Y_{E_1,X} + Y_{E_2,X}] + (\alpha - 1)Y_{M,X}}{Y_{M,X}} \qquad (12b)$$

The absolute intensities of some very unsaturated ions were found to be independent of molecular weight. This is obtained for $n > 2$ when A' is close to zero and these ions do not undergo any end group interaction for promoting their formation ($Y_{E_1,X} = Y_{E_2,X} = 0$; $\alpha = 1$). Nevertheless, we are not able to detect the decrease of the absolute intensities expected at very low molecular weight. Indeed, with a standard deviation of 10% for the absolute intensities (in practice it can exceed this value), the decrease for Y_X will be meaningful only for polymers containing less than 18 repeat units.

The upper limit of validity for this model is $m/z = 105$ owing to the fact that each "linked molecule" contains only one repeat unit. Nevertheless, this model can be easily extended to heavier ions (above $m/z = 105$) by taking two (or more) repeat units in one "linked molecule" (see E_1', E_2', and M_i' in Scheme 2). Then the number of "molecules" in the macrochain with *n* repeat units becomes $n - 1$.

Equation 12 becomes

$$Y_X = \frac{1}{n+1}A'' + \frac{n}{n+1}B \qquad (13)$$

with, for a high molecular weight polymer,

$$\lim_{n\to\infty} Y_X = Y_{M,X} = B$$

In this case, the minimum number of repeat units that the smaller molecules should contain is one:

$$\lim_{n\to 1} Y_X = \frac{1}{2}[Y_{E_1,X} + Y_{E_2,X}] + \frac{(\alpha - 2)}{2}Y_{M,X} = A''$$

The ratio A''/B is still related to the extent of the end group interaction and is similar to A'/B. Equation 13 is of the same type as (12).

In most cases of the literature, the intensity ratio between a specific ion (E_1) of the end group and a main chain ion X_2 is used. With our model, it becomes, using the same assumptions as in eq 10,

$$\frac{Y_{E_1}}{Y_{X_2}} = \frac{1}{(n - 1 + \alpha)}\frac{Y_{E_1,E_1}}{Y_{M,X_2}} \qquad (14)$$

and more generally

$$\frac{Y_{E_1}}{Y_{X_2}} = \frac{Y_{E_1,E_1}}{Y_{E_1,X_2} + Y_{E_2,X_2} + (n - 1 + \alpha)Y_{M,X_2}} \qquad (15)$$

For this last equation, we can calculate the limits as was done for eq 11 and the same equation is obtained for the A'/B ratio (eq 12b).

The experimental intensities are well fitted with eq 12, as shown for the C_8 cluster by the solid lines in Figure 5. The A'/B ratios obtained from the two fitting parameters are presented in Figure 8 for the first data set (s* in Table 1). Only values for which the correlation coefficient is higher than 0.93 are indicated. Since the A'/B (A''/B) values for very dehydrogenated ions are close to zero, they are not presented in the figure. It may be seen that the ratio A'/B ratio increases periodically in each cluster when the ion hydrogen content increases. The A'/B ratio increase indicates that the end group interaction (E_1 or E_2) becomes more and more active to promote the more hydrogenated ions. Within each cluster, the H exchange increases when m/z increases. Moreover, the A/B value for I_{TOTAL} is 16.5.

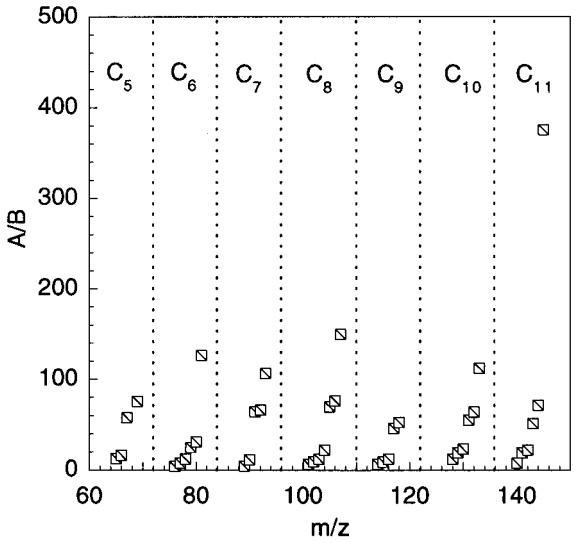

Figure 8. End group interaction ratio (A'/B and A''/B) for the PS SIM spectrum with m/z from 60 to 160.

The results show that the ion formation pathways from a given precursor are dependent on its adjacent functionality in the chain. The SIMS sensitivity of one specific chemical functionality is then dependent on its neighboring and linked chemical groups. This may explain why the quantification of the different functionalities of the copolymers is very difficult to achieve when it is based on a limited number of peak intensities (two or three). Indeed, these peaks have to be chosen with care in order to avoid interactions with the adjacent groups. Then a linear relationship between secondary ion intensities and the surface sample content can be found, as, for example, in the case of the styrene–butadiene random copolymer.[26]

Conclusion

The molecular weight is shown to influence most of the ion intensities when it is lower than 10^4. Above this limiting value, constant intensities were found. This limit can be modified if a preferential segregation of the end group occurs.

When the normalized intensities are considered, three types of ion intensity behavior are observed when varying the molecular weight whatever the end group: some ion intensities increase at low molecular weight, some others are nearly constant in the investigated M_n range, and some others are decreasing at low molecular weight. This decrease is only due to the normalization procedure. Indeed, their absolute intensities remain constant. This shows the difficulty of applying normalization procedures to the SIMS spectra.

These molecular weight effects on the polystyrene SIMS spectra are explained on the basis of new fragmentation pathways due to the interactions between the first repeat unit and the end group. This interaction favors the formation of more hydrogenated ions by a H transfer. The end groups also have an influence on the other PS characteristic peaks, which needs some reor-

ganization of the polymer chain before their formation (i.e., the tropylium ion).

The structure of the end group (*n*-, *sec*-, and *tert*-butyl) has a major effect on the ion intensities of the low molecular weight polystyrene. First, the intensity of the peak related to the butyl end groups (57 *m*/*z*, $C_4H_9^+$), increases as the stability of the formed ion (stabilization by resonant or inductive effects). Second, the structure of the end groups has a strong effect on the main chain ion intensities for the low molecular weight (<10000) PS. The hydrogen exchange does not seem to exist for *tert*-butyl samples.

A model is proposed to account for the influence of the end group on the fragmentation pattern of polystyrene samples. It describes correctly the ion absolute intensity dependencies. The fit of the model parameters allows us to quantify the H transfer from the end group, which increases with the H content in each C cluster.

Acknowledgment. The financial support from the "Fonds National de la Recherche Scientifique (FNRS)-Loterie Nationale" (Belgium) and from the "Région Wallonne" (Belgium) for the acquisition of the ToF-SIMS spectrometer is gratefully acknowledged. The authors thank Dr. P. Dubois (CERM, Center for Education and Research on Macromolecules) for his help in providing some of the samples and Pr. J. P. Issi and Mrs V. Wiertz for helpful discussions.

References and Notes

(1) (a) Benninghoven, A. *Angew. Chem., Int. Ed. Engl.* **1994**, *33*, 1023. (b) Gardella, J. A.; Pireaux, J. J. *Anal. Chem.* **1992**, *60*, 645A. (c) Vickerman, J. C. *Analyst* **1994**, *119*, 513. (d) van Leyen, D.; Hagenhoff, B.; Niehuis, E.; Benninghoven, A.; Bletsos, I. V.; Hercules, D. M. *J. Vac. Sci. Technol. A* **1989**, *7* (3), 1790. (e) Briggs, D. *Surf. Interface Anal.* **1982**, *4*, 151. (f) Short, R. D.; Ameen, A. P.; Jackson, S. T.; Pawson, D. J.; O'Toole, L.; Ward, A. J. *Vacuum* **1993**, *44*, 1143.

(2) (a) Newman, J. G.; Carlson, B. A.; Michael, R. S.; Moulder, J. F.; Holt, T. H. *Static SIMS Handbook of Polymer Analysis*; Perkin-Elmer Corp.: Eden Prairie, MN, 1991. (b) Briggs, D.; Brown, A.; Vickerman, J. C. *Handbook of Static Secondary Ion Mass Spectrometry (SIMS)*; John Wiley & Sons: New York, 1989.

(3) Delcorte, A.; Bertrand, P.; Arys, X.; Jonas, A.; Wischeroff, E.; Mayer, B.; Laschewsky, A. *Surf Sci.* **1996**, *366*, 149.

(4) Williams P. Ion and Neutral Spectroscopy. In *Practical Surface Analysis*, 2nd ed.; Briggs, D., Seah M. P., Eds; John Wiley & Sons: Chichester, U.K., 1992; Vol. II, p 197.

(5) Leggett, G. J.; Vickerman, J. C.; Briggs, D.; Hearn, M. J. *J. Chem. Soc., Faraday Trans.* **1992**, *88*, 297.

(6) Delcorte, A.; Bertrand, P. In *10th International Conference on Secondary Ion Mass Spectrometry SIMS X*; Benninghoven, A., Hagenhoff, B., Werner, H. W., Eds.; J. Wiley & Sons: New York, 1997; p 731.

(7) Leggett, G. J.; Vickerman, J. C. *Int. J. Mass Spectrom. Ion Processes* **1992**, *122*, 281.

(8) Chilkoti, A.; Castner, D. G.; Ratner, B. D. *Appl. Spectrosc.* **1991**, *45* (2), 209.

(9) Affrossman, S.; Hartshorne, M.; Jérôme R.; Munro, H.; Pethrick, R. A.; Petitjean, S.; Vilar, M. R. *Macromolecules* **1993**, *26*, 5400.

(10) Muddiman, D. C.; Brockman, A. H.; Proctor, A.; Houalla, M.; Hercules, D. M. *J. Phys. Chem.* **1994**, *98*, 11570.

(11) Belu, A. M.; Hunt, M. O., Jr.; DeSimone, J. M.; Linton, R. W. *Macromolecules* **1994**, *27*, 1905.

(12) Vanden Eynde, X.; Weng, L. T.; Bertrand, P. In *10th International Conference on Secondary Ion Mass Spectrometry SIMS X*; Benninghoven, A., Hagenhoff, B., Werner, H. W., Eds.; J. Wiley & Sons: New York, 1997; p 727.

(13) Shard, A. G.; Volland, C.; Davies, M. C.; Kissel, T. *Macromolecules* **1996**, *29*, 748.

(14) Reihs, K.; Kircher, K.; Deimel, M.; Voetz, M.; Petrat, F. M.; Wolany, D.; Benninghoven, A. In *10th International Conference on Secondary Ion Mass Spectrometry SIMS X*; Benninghoven, A., Hagenhoff, B., Werner, H. W., Eds.; J. Wiley & Sons: New York, 1997; p 641.

(15) (a) Hittle, L. R.; Proctor, A.; Hercules, D. M. *Macromolecules* **1995**, *28*, 6238. (b) Hittle, L. R.; Proctor, A.; Hercules, D. M. *Anal. Chem.* **1994**, *66*, 108.

(16) Leeson, A. M.; Alexander, M. R.; Short, R. D.; Briggs, D.; Hearn, M. J. *Surf. Interface Anal.* **1997**, *25*, 261.

(17) Vanden Eynde, X.; Fallais, I.; Devaux, J.; Bertrand, P. ICPSI-2 Conference Proceedings (Namur-Belgium, 1996), in press.

(18) Painter, P. C.; Coleman, M. M. *Fundamentals of Polymer Sciences*, **1994**, Technomic Publishing.

(19) Weng, L. T.; Bertrand, P. *Mikrochem. Acta* **1996**, *13*, 167.

(20) See part II in this paper.

(21) Affrossman, S.; Hartshorne, M.; Jérôme, R.; Pethrick, R. A.; Petitjean, S.; Vilar, M. R. *Macromolecules* **1993**, *26*, 6251.

(22) McLafferty, F. W. *Interpretation of Mass Spectra*, 4th ed.; University Science Books: Mill Valley, CA, 1993.

(23) Castner, D. G.; Ratner, B. D. *Surf. Interface Anal.* **1990**, *15*, 479.

(24) Benninghoven, A. *Angew. Chem., Int. Ed. Engl.* **1994**, *33*, 1023.

(25) Vanden Eynde, X.; Reihs, K.; Bertrand, P. In *11th International Conference on Secondary Ion Mass Spectrometry SIMS XI*, in press.

(26) Weng, L. T.; Bertrand, P.; Lauer, W.; Zimmer, R.; Busetti, S. *Surf. Interface Anal.* **1995**, *23*, 879.

(27) Lias, S. G.; Bartmess, J. E.; Liebman, J. F.; Holmes, J. L.; Levin, R. D.; Mallard, W. G. *Gas Phase Ion and Neutral Thermochemistry*; American Chemical Society, American Institute of Physics, National Bureau of Standards: Washington, DC, 1988; p 163.

MA9702049